Comparison between 5,10,15,20-Tetraaryl- and 5,15-Diarylporphyrins as Photosensitizers: Synthesis, Photodynamic Activity, and Quantitative Structure−Activity Relationship Modeling

Stefano Banfi,* Enrico Caruso, Loredana Buccafurni, Roberto Murano, Elena Monti, Marzia Gariboldi, Ester Papa, and Paola Gramatica

Department of Structural and Functional Biology, University of Insubria, Via H. Dunant 3, 21100 Varese (VA), Italy

Received October 6, 2005

The synthesis of a panel of seven nonsymmetric 5,10,15,20-tetraarylporphyrins, 13 symmetric and nonsymmetric 5,15-diarylporphyrins, and one 5,15-diarylchlorin is described. In vitro photodynamic activities on HCT116 human colon adenocarcinoma cells were evaluated by standard cytotoxicity assays. A predictive quantitative structure−activity relationship (QSAR) regression model, based on theoretical holistic molecular descriptors, of a series of 34 tetrapyrrolic photosensitizers (PSs), including the 24 compounds synthesized in this work, was developed to describe the relationship between structural features and photodynamic activity. The present study demonstrates that structural features significantly influence the photodynamic activity of tetrapyrrolic derivatives: diaryl compounds were more active with respect to the tetraarylporphyrins, and among the diaryl derivatives, hydroxy-substituted compounds were more effective than the corresponding methoxy-substituted ones. Furthermore, three monoarylporphyrins, isolated as byproducts during diarylporphyrin synthesis, were considered for both photodynamic and QSAR studies; surprisingly they were found to be particularly active photosensitizers.

Introduction

Photodynamic therapy (PDT) is a minimally invasive treatment that uses the combination of a photosensitizing agent (PS) and light to selectively target solid tumors, as well as several nonneoplastic proliferating cell diseases. Systemic administration of the PS is followed by localized irradiation with visible light; in the presence of adequate concentrations of molecular oxygen, PS photoactivation results in the formation of reactive oxygen species (ROS) and related tissue damage.[1,2]

The first PS to be granted regulatory approval (in Canada, 1993) was porfimer sodium (Photofrin), a purified form of hematoporphyrin derivative consisting of a mixture of porphyrins. Porfimer sodium is currently used in more than 40 countries worldwide to treat a variety of cancers, including cancers of the lung, stomach, cervix, and bladder and esophageal adenocarcinoma. However, despite its continuing effectiveness, porfimer sodium has a number of disadvantages, most notably low tissue penetration of activating light (due to its weak absorption at 630 nm), extended skin photosensitivity, and low selectivity between tumor and healthy tissue in the early phases of treatment, and this has spurred an active search for novel ("second-generation") PSs with improved properties over the past 20 years. Most second-generation PSs (such as chlorins, bacteriochlorins, and phthalocyanines) belong to the tetrapyrrole class; while many agents have been identified with better absorption at longer wavelengths than porfimer sodium, thereby increasing the depth at which photodynamic cell kill can be achieved, only one second-generation PS, the 5,10,15,20-tetrakis(*m*-hydroxyphenyl)chlorin (*m*-THPC or temoporfin, currently marketed as Foscan) has been recently approved for the palliative treatment of head and neck cancer, and the quest for novel candidates is still ongoing.

Among porphyrins/chlorins, compounds bearing aromatic substituents only at the 5 and 15 positions of the tetrapyrrolic ring are particularly attractive, as they combine some features of the 5,10,15,20-tetraaryl derivatives (characterized by unsubstituted β-pyrrole positions) with those of the β-pyrrole octaalkylporphyrins [bearing a hydrogen atom at each 5,10,15,20 position (meso) of the tetrapyrrolic ring]. A large number of structural modifications, including bromination, nitration, or formylation, can be performed at the free 10,20-positions, which makes 5,15-diarylporphyrins suitable for such diverse applications as light-harvesting antenna systems,[3] liquid crystal porphyrins,[4] and nonlinear optical devices.[5] To date, only scattered reports have been published on the potential use of 5,15-diaryporphyrins or chlorins as PSs.[6] Following up on the recent development by our group of a series of tetrapyrrole derivatives with potential use in medicine,[7] the present study reports the synthesis of a panel of novel tetraaryl- and diarylporphyrins and their in vitro photodynamic activities against the cultured human colon adenocarcinoma cell line HCT116. Quantitative structure−activity relationship (QSAR) analysis was performed on a larger set of PSs, including the newly synthesized derivatives and the monoarylporphyrin byproducts, as well as previously reported symmetric compounds.[7]

Results and Discussion

A series of tetraaryl- and diarylporphyrins was synthesized, based on the assumption that the presence of phenyls with different substituents at the meso positions would affect the hydrophobic/hydrophilic character of the resulting PSs. This is a crucial feature for both cell penetration and subcellular localization, and it is generally believed that amphiphilic molecules, bearing both hydrophobic and hydrophilic moieties, display improved tumor-selective uptake and retention, particularly when polar and nonpolar groups are distributed nonsymmetrically.[8]

Chemistry. Nonsymmetric tetraarylporphyrins (**1**−**7**) (Figure 1) were synthesized via acid-catalyzed mixed condensation of pyrrole with two different aromatic aldehydes, following the general procedure described by Lindsey and co-workers.[9] The porphyrinogen intermediate was then oxidized to porphyrin with

* To whom correspondence should be addressed: phone +39-0332-421550; fax +39-0332-421554; e-mail stefano.banfi@uninsubria.it.

10.1021/jm050997m CCC: $33.50
Published on Web 04/29/2006

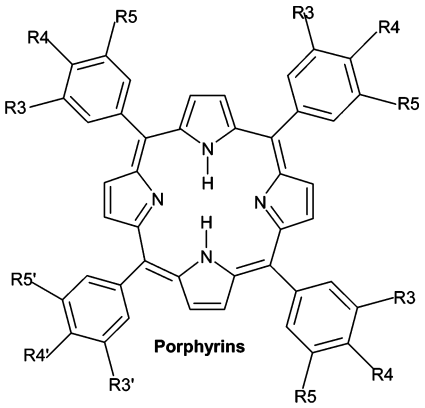

Porphyrins	R3	R4	R5	R3'	R4'	R5'
1	H	H	H	H	OCH_3	H
2	H	H	H	OCH_3	H	H
3	H	H	H	OCH_3	OCH_3	OCH_3
4	H	OCH_3	H	OCH_3	OCH_3	OCH_3
5	H	H	H	H	OH	H
6	H	H	H	OH	H	H
7	H	H	H	OH	OH	OH

Figure 1. Structures of tetraarylporphyrins **1**−**7**.

2,3-dichloro-5,6-dicyano-1,4-benzoquinone (DDQ). The yields of the recovered products range between 10% and 20%.

A number of different procedures have been reported for the synthesis of 5,15-diarylporphyrins,[10] mostly based on a (2 + 2)-type condensation in which two dipyrrolic compounds incorporating one type of carbon bridge are fused together, thereby forming the other type of carbon bridge; the intermediate is then oxidized in situ to the final porphyrin. While in principle there are many (2 + 2)-type synthetic pathways to obtain 5,15-diarylporphyrins,[10a] the most frequently reported procedures rely on condensation of 5-aryldipyrromethane with a second moiety of 1,9-functionalyzed dipyrromethane.[11] For the present study, after a few preliminary attempts, we found that better overall yields could be obtained when 5-unsubstituted dipyrromethane was reacted with aromatic aldehydes, following the procedure described by Plater et al.[12] Accordingly, pyrrole was reacted with thiophosgene to give the di-2-pyrrolylthione, which was then oxidized with 30% hydrogen peroxide to the corresponding ketone; the final reduction with $NaBH_4$ produces the desired dipyrromethane. Attempts to carry out direct hydrodesulfurization of thione group with $LiAlH_4$ or $NaBH_4$ did not afford the desired product in appreciable yields.

Acid-catalyzed condensation of dipyrromethane with desired aromatic aldehydes afforded a series of 5,15-diarylporphyrins (**8**−**20**), isolated with a variable yields from 10% to 25% (Figure 2).

Interestingly, under the experimental conditions adopted, in a few peculiar cases the reaction between dipyrromethane and aromatic aldehyde generated a side product that was recognized as the monoarylporphyrin. To date, we have not been able to establish the actual mechanism leading to the formation of this product; most probably, methylene units provided by dipyrromethane allow the closure of the tetrapyrrolic ring with only one aldehyde unit. For the sake of comparison, the monoarylporphyrins serendipitously isolated during diarylporphyrin synthesis (**22**−**24**) (Figure 3) were also included in the in vitro study of photodynamic activity performed in HCT116 cells; to the best of our knowledge, only one paper has appeared to date assessing monosubstituted tetrapyrroles as potential PSs.[13]

To confirm our previous results about the relationship between the photodynamic activity of porphyrins and that of the corresponding chlorin derivatives,[7] we also synthesized the chlorin **21**, obtained from the corresponding diarylporphyrin **8** by the diimide reduction method.[14]

Photobleaching. It is known that tetrapyrrolic compounds undergo partial demolition in the presence of oxidizing species, and it is generally believed that bleaching can be mediated by singlet oxygen,[15a] although some experiments suggest that radical-mediated photodegradation (type I) predominates.[15b] To select an appropriate irradiation time for cytotoxicity studies, we assessed the rate of photodegradation for the new compounds (Figure 4), based on the decreasing intensity of the Soret band. Our main concern here was that diaryl derivatives, characterized by the presence of unsubstituted meso positions that can undergo fast oxidation, might be largely photodegraded during irradiation of the cells; furthermore, these assays allowed us to compare the degradation rates of methoxy- and hydroxy-substituted porphyrins, which, in principle, could exhibit different behaviors upon irradiation. However, no significant differences were observed among the three classes of PSs, namely, tetra-, di-, and monoarylporphyrins, as well as between hydroxy- and methoxyphenyl-substituted porphyrins; for most compounds approximately 60% of the intensity of the initial Soret band was maintained following 2 h exposure to a 500 W tungsten−halogen lamp. The stability of temoporfin and porfimer sodium was also assessed under these conditions; both compounds showed a comparable extent of photobleaching. It may be worth emphasizing that, to allow the UV−vis spectral determination at 400−420 nm, the PS concentrations used in these experiments (5×10^{-5} M) were significantly higher than those used for PDT on cell cultures (nanomolar range); thus, it is reasonable to hypothesize that, in the low PS concentration range used for PDT experiments, the extent of photobleaching may be even lower.

Cytotoxicity Assays. The IC_{50} values from dose/response curves obtained in HCT116 cells following exposure to the different PSs for 24 h and irradiation with visible light for 2 h are reported in Table 1; porfimer sodium and temoporfin were also included as reference compounds. The intrinsic cytotoxicity of PSs was assessed by omitting the irradiation step from the treatment protocol and was found to be negligible in all cases up to PS concentrations 10-fold higher than those used for PDT experiments.

All the diaryl compounds tested in the present study were significantly more effective than the corresponding tetraaryl derivatives; in fact, the range of IC_{50} values obtained for diarylporphyrins was 1.06−52.46 nM (median 9.84 nM) versus 53.31−1886.79 nM (median 344 nM) for tetraaryl derivatives. The most effective diaryl compound tested **19** was also significantly more phototoxic than both porfimer sodium and temoporfin (IC_{50} values: compound **19**, 0.51 ± 0.07 ng/mL; porfimer sodium, 73.67 ± 8.04 ng/mL; temoporfin, 5.17 ± 0.39 ng/mL; concentrations are expressed in nanograms per milliliter because an exact molecular weight cannot be calculated for porfimer sodium, which is a mixture of oligomers).

Cytotoxicity data reported in Table 1 indicate that hydroxy-substituted porphyrins are significantly more effective that the corresponding methoxy derivatives, thus confirming our previ-

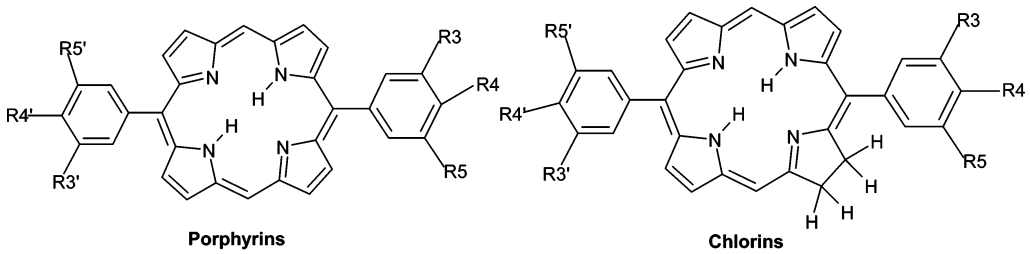

Porphyrins	R3	R4	R5	R3'	R4'	R5'
8	H	H	H	H	H	H
9	H	OCH_3	H	H	OCH_3	H
10	OCH_3	H	H	OCH_3	H	H
11	OCH_3	OCH_3	OCH_3	OCH_3	OCH_3	OCH_3
12	H	H	H	H	OCH_3	H
13	H	H	H	OCH_3	H	H
14	H	H	H	OCH_3	OCH_3	OCH_3
15	H	OCH_3	H	OCH_3	OCH_3	OCH_3
16	OCH_3	H	H	OCH_3	OCH_3	OCH_3
17	H	OH	H	H	OH	H
18	H	H	H	H	OH	H
19	H	H	H	OH	H	H
20	H	H	H	OH	OH	OH
Chlorin	**R3**	**R4**	**R5**	**R3'**	**R4'**	**R5'**
21	H	H	H	H	H	H

Figure 2. Structures of diarylporphyrins **8**−**20** and of chlorin **21**.

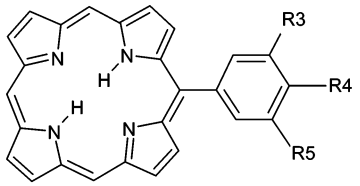

Porphyrins	R3	R4	R5
22	H	H	H
23	H	OCH_3	H
24	OCH_3	OCH_3	OCH_3

Figure 3. Structures of monoarylporphyrins **22**−**24**.

ous findings.[7] It may be worth mentioning that mono- or disubstitution of the phenyl rings with hydroxyl groups generally yields good photodynamic agents: in temoporfin, the most active compound currently in clinical use, all four phenyl rings bear a hydroxyl group in the meta position; in addition, Patrice and co-workers[6b] recently reported on a promising diaryl PS again bearing four hydroxyl groups (two for each phenyl ring). As mentioned above, the different activities of hydroxyl and methoxy derivatives cannot be accounted for by different intrinsic cytotoxicities or different photodegradation rates. A tentative explanation for the better photodynamic performance of hydroxyl-substituted porphyrins could depend on their greater solubility in the aqueous medium. Unfortunately, we were unable to obtain experimental data to support this hypothesis, as the octanol/water partition coefficients could not be determined for most of the agents in this study, due to their highly lipophilic nature, yielding concentrations in the aqueous phase that were below the limits of detection (even when the aqueous phase was in 10-fold excess to the octanol layer). On the basis of log *P* values calculated according to different computational approaches (Table 2 in Supporting Information), a small difference can be detected between the hydroxyl-substituted and the corresponding methoxy-substituted porphyrins, as expected from the effect of a few small polar groups on a large hydrocarbon skeleton. The slightly more hydrophilic nature of

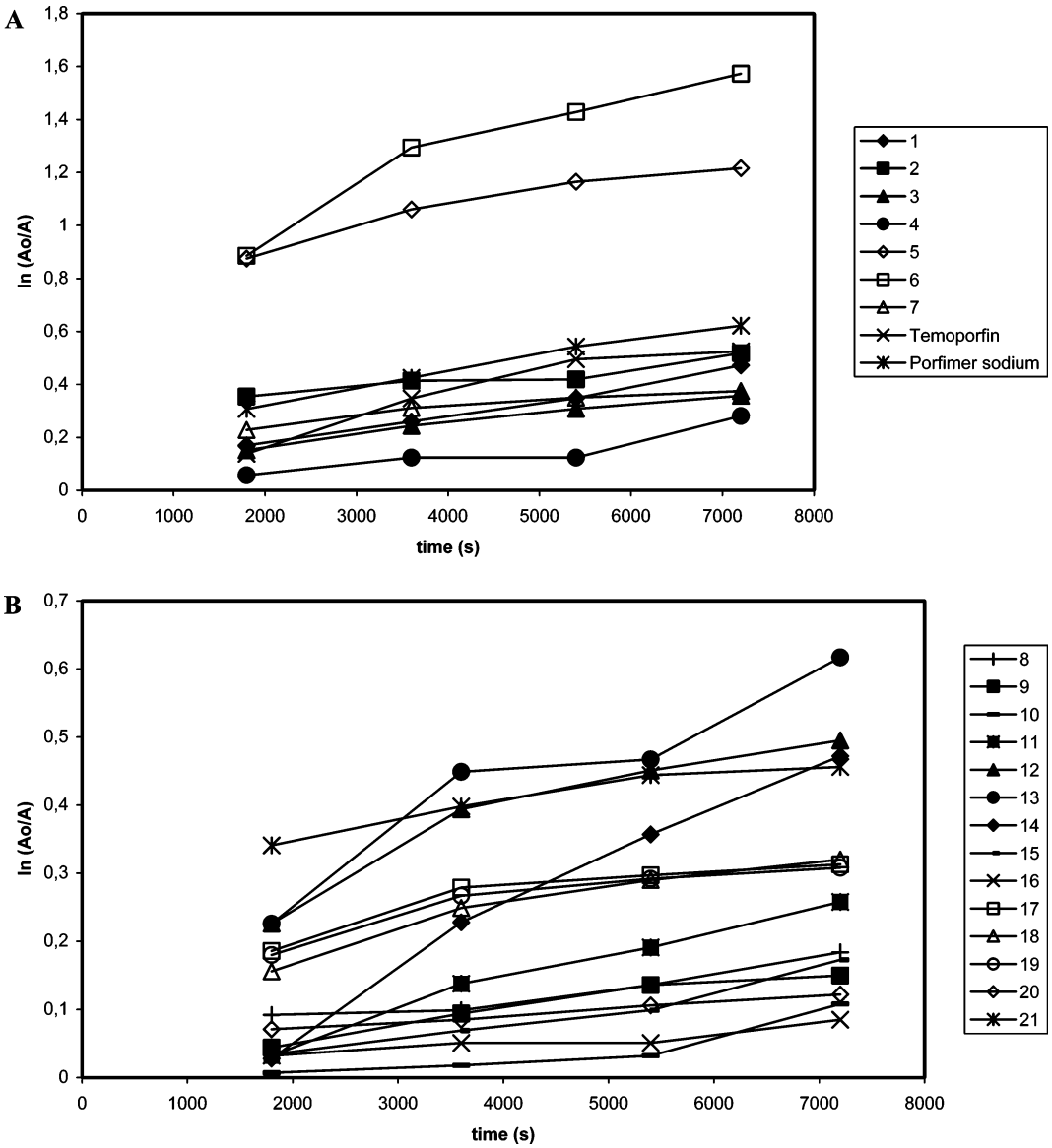

Figure 4. Photobleaching of tetraarylporphyrins (A) and diaryl- and monoarylporphyrins (B).

hydroxy-substituted derivatives might concur with other, as yet unidentified factors, to the observed difference in photodynamic activity.

The fact that we decided to perform the present study on porphyrins, despite the higher in vivo activity of chlorins, deserves some comments. The better in vivo performance of chlorins can be attributed to their absorbance profile at longer wavelengths as compared to the corresponding porphyrins, allowing photoactivation of the PS at greater depths within the irradiated tissues. Significant differences in cellular uptake or subcellular distribution between chlorins and the corresponding porphyrins, which could result in different activities, have never been reported. Accordingly, results obtained for compounds **8** and **21** (diphenylporphyrin and the corresponding chlorin derivative) indicate a nonsignificant difference between the phototoxic activities of the two compounds (5.66 ± 1.16 nM for the porphyrin vs 3.26 ± 2.06 nM for the chlorin). These data, together with previously reported observations by our group,[7] indicate that a good correlation exists between the photodynamic effects of porphyrins and those of the corresponding chlorins. In addition, the synthesis of porphyrins is straightforward and gives better yields, due to the greater stability of the totally unsaturated skeleton, as compared to the reduced form of chlorins,[16] thus providing a further rationale for the use of porphyrins instead of chlorins for in vitro screens of photodynamic activity. Once the best lead compounds have been identified, conversion to the corresponding chlorins will yield active PSs more suitable for in vivo applications.

Finally, an interesting finding regards the phototoxicity of the serendipitously isolated monoaryl derivatives (**22**−**24**), with IC_{50} values ranging between 1.85 and 4.8 nM (median 3.2 nM); further studies will specifically address the photodynamic properties of this promising series of compounds.

QSAR Analysis. To the best of our knowledge, very few QSAR analyses of photosensitizers for photodynamic therapy[17−19] have been published. Two QSAR models[17,18] are based on the octanol/water partition coefficient and simple structural elements, such as length and shape of alkyl chains, while the more recent paper[19] applies theoretical molecular descriptors in multiple linear regression (MLR) and artificial neural network (ANN) models of only 12 pyropheophorbides. A previous 3D-QSAR model, based on CoMFA and PLS, was published by Debnath et al.[20] for the modeling of 21 porphyrin derivatives, including meso-unsubstituted and tetraaryl-substituted porphyrins, with anti-HIV-1 activity. The model had a low predictivity ($Q^2 = 0.59$), verified just by leave-one-out cross-validation,

Table 1. IC_{50} Values[a] for the Tested Compounds

molecule	IC_{50}, ng/mL ± SE	IC_{50}, nM ± SE
porfimer sodium	73.67 ± 8.04	
temoporfin	5.17 ± 0.39	7.60 ± 0.57
	Tetraarylporphyrins	
1	893.76 ± 44.73	1386.97 ± 69.42
2	99.80 ± 1.21	154.88 ± 1.88
3	708.52 ± 137.13	1006.14 ± 194.73
4	>1500	>1886.79
5	145.03 ± 24.52	230.06 ± 38.90
6	216.87 ± 17.02	344.03 ± 27
7	35.30 ± 7.57	53.31 ± 11.43
	Diarylporphyrins	
8	2.63 ± 0.54	5.66 ± 1.16
9	27.39 ± 1.51	52.46 ± 2.89
10	12.92 ± 0.97	24.74 ± 1.85
11	6.32 ± 0.35	9.84 ± 0.54
12	6.06 ± 0.53	12.31 ± 1.07
13	2.93 ± 0.42	5.94 ± 0.85
14	4.28 ± 1.30	7.75 ± 2.36
15	9.03 ± 2.49	15.51 ± 4.27
16	9.21 ± 2.69	15.81 ± 4.62
17	3.51 ± 1.26	7.09 ± 2.54
18	3.35 ± 0.10	7.01 ± 0.21
19	0.51 ± 0.07	1.06 ± 0.15
20	4.97 ± 0.38	9.75 ± 0.74
21	1.51 ± 0.96	3.26 ± 2.06
	Monoarylporphyrins	
22	1.23 ± 0.29	3.2 ± 0.76
23	0.77 ± 0.29	1.85 ± 0.71
24	2.29 ± 0.14	4.8 ± 0.29

[a] Porphyrin concentrations inhibiting tumor cell growth by 50%. IC_{50} value are reported as means of three independent replications ± SE (standard error).

probably due to a high degree of heterogeneity of the structures of the molecules in the panel. In the present paper, 34 chemicals, including the newly synthesized PSs described above along with previously reported ones,[7] were tested for their photodynamic activity, to develop a validated MLR QSAR model, based on theoretical molecular descriptors for this specific chemical domain. In addition, the size of the available data set allows statistical external validation of the model as well as the more common internal validation. Assessing the predictivity of the chemical applicability domain of the proposed model, that is, the ability of the model to yield reliable data, is crucial for application of the model to the design of novel, more effective derivatives belonging to the verified chemical domain.

QSAR model development was performed by the procedure described in the Experimental Section. A wide set of theoretical molecular descriptors[21] was used as input set of variables for modeling, to identify different structural features of the PSs related to the relevant effect (i.e., photodynamic activity). Different kinds of calculated log *P* (*A* log *P*,[21] *M* log *P*,[21] and HYPER-log *P*[22]) were also used as input variables during model development.

As we cannot know a priori which descriptors could be related to photodynamic activity and therefore useful in models for prediction, we applied an evolutionary variable selection procedure (genetic algorithms,[23] GA-VSS) to select only the best combinations of descriptors most relevant to obtaining models with the highest predictive power for photodynamic cytotoxicity.

In addition to different internal validation procedures (leave-one-out, bootstrap, and Y-scrambling), for a stronger and more reliable evaluation of model applicability for the prediction on new chemicals,[24] statistical external validation of the models was also performed by randomly splitting [in connection with the response values, log ($1/IC_{50}$)] the available experimental set of 34 chemicals (24 reported in this work and 10 in previous work[7]) into 22 training chemicals for model development and 12 validation chemicals for model evaluation. The model with the highest external predictivity (verified by Q^2_{ext}) was selected in the GA population of models, each based on various combinations of different descriptors, and it is proposed here as the reference QSAR for log ($1/IC_{50}$) calculations.

The best predictive three-variable MLR model has the following equation and statistical parameters:

$$\log 1/IC_{50} = -10.06(\pm 3.89) + 21.05(\pm 2.31)\text{GATS6v} - 40.55(\pm 8.27)\text{PW3} + 36.15(\pm 13.71)\text{R4u+} \quad (1)$$

where $n_{training} = 22$, $n_{validation} = 12$, $R^2 = 0.86$, $Q^2 = 0.81$, $Q^2_{boot} = 0.80$, $Q^2_{ext} = 0.77$, $s = 0.388$, $F = 36.49$, $K_{xx} = 18.9$, $K_{xy} = 40.8$, RMSE = 0.41, and RMSEP = 0.46. The reported fitting and validation parameters have high values, indicating that the model is stable and has very good descriptive (R^2) and predictive performance (Q^2). The quality of Q^2_{ext} (0.77) and the small RMSE and RMSEP values (similar for training and validation sets) confirm the robustness and good predictivity of this model.

The model is dominated by the autocorrelation descriptor GATS6v (Geary autocorrelation, of lag 6, weighted by the atomic van der Waals volumes)[25,26] (standardized regression coefficient 0.83), which accounts for the correlation among atoms, weighted by the van der Waals volumes, with a distance of six bonds (the lag) in the molecule; GATS6v is a distance-type function and gives mainly information on the molecular size. The second most informative descriptor is the topological descriptor PW3 (path/walk 3-Randic shape index)[27] (standardized regression coefficient −0.45) mainly accounting for molecular shape information, whereas the least relevant descriptor is the GETAWAY descriptor[28] R4u+ (standardized regression coefficient 0.25), the maximal value of autocorrelation descriptor (atoms individually weighted, topological distance of four bonds) based on the influence/distance matrix, which takes into account local structural aspects of the molecules. Thus, the size and shape features, described by specific molecular descriptors in their multivariate combination, are selected as the dominant structural aspects related to the photodynamic activity of the set of PSs examined in the present study.

It is noteworthy that models developed on the basis of calculated log *P* (*A* log *P*, *M* log *P*, HYPER-log *P*) as a single descriptor were unpredictive as regards the whole set of 34 compounds. In particular, the sulfonamido compounds **31** and **32** fall totally outside the domain; however, even without considering the two sulfonamido compounds, log *P*-based models developed on the remaining 32 chemicals had the following unsatisfactory statistical parameters: for *A* log *P*, $R^2 = 0.57$ and $Q^2_{loo} = 0.51$; for *M* log *P*, $R^2 = 0.06$ and $Q^2_{loo} = -0.27$; and for HYPER-log *P*, $R^2 = 0.45$ and $Q^2_{loo} = 0.38$. The QSAR model proposed here highlights the ability of the selected molecular descriptors to identify the structural aspects related to the photodynamic activity, whereas models based on log *P* alone are unable to capture this information of this set of porphyrins. In addition, it is important to remember that, in apparent contradiction to its widespread use, log *P* is not a universal descriptor and its value is strongly variable depending on the experimental procedure or the calculation method applied.[29−31] The GA population of models developed by adding various log *P* to the previously selected theoretical molecular descriptors (Table 2) have lower robustness and worse

Table 2. Models Developed Including Various Calculated Log *P* Values in Addition to Theoretical Descriptors

variables	R^2	Q^2	Q_{boot}^2	Q_{ext}^2	K_x, %	K_{xy}, %
PW3, GATS6v, R4u+	0.86	0.81	0.80	0.77	18.90	40.77
PW3, GATS6v, HYPER-log *P*	0.81	0.77	0.68	0.52	32.83	49.30
PW3, GATS6v, *A* log *P*	0.80	0.74	0.72	0.49	35.32	50.29
PW3, GATS6v, *M* log *P*	0.81	0.65	0.43	0.49	21.01	41.44
GATS6v, R4u+, *A* log *P*	0.74	0.64	0.54	0.82	25.40	43.77
GATS6v, R4u+, HYPER-log *P*	0.72	0.49	0.42	0.64	31.71	39.36
GATS6v, R4u+, *M* log *P*	0.67	0.22	0.28	0.61	25.10	36.75

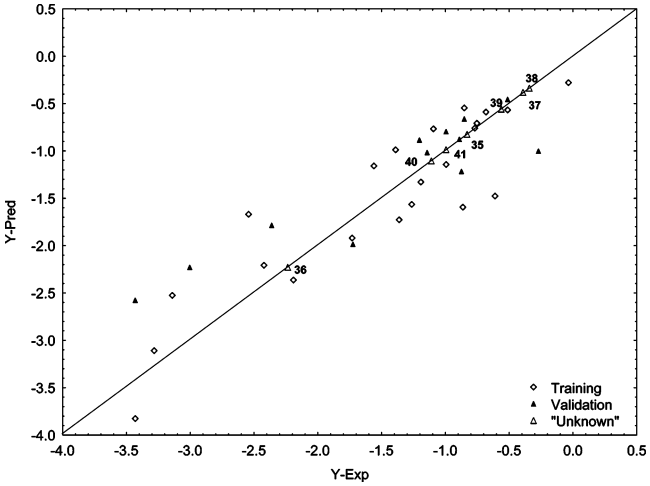

Figure 5. Regression line of the proposed QSAR model. The training and validation chemicals are differently labeled and the "unknown" chemicals are also numbered.

performance, mainly in external predictivity, than the model proposed here (eq 1).

The regression line of the QSAR model presented above is reported in Figure 5, where it is possible to observe the good and balanced distribution of the validation set into the training set, highlighting the efficacy of the splitting.

The analysis of the chemical applicability domain of the model with the leverage approach[32,33] allows us to verify the presence of outliers for the response or chemicals influential for some peculiarities in their structure. In general, all the chemicals are well predicted (residuals within 2.5 standard deviations) and are also within the structural applicability domain (into the leverage value of hat). It is also important to note that the validation chemicals, which were not used for model development, are predicted with similar accuracy as the training chemicals. The QSAR model was also used to predict the activities of five as yet unknown porphyrins (**37**−**41**), of the parent porphyrin tetraphenyl derivative (**36**) and of the diarylchlorin **35**, recently reported by the Patrice group[6b] (Figure 6).

We have also verified by the leverage that these unknown compounds are also within the structural chemical domain of the model; thus their predicted data should be considered not as extrapolated from the model but as reliable predictions.

This part of the study was performed with two aims: (a) to verify the model predictivity on the well-known compound **36** and on porphyrin **35**, independently described by other authors as a very active photosensitizer, and (b) to obtain indications on the biological activity of newly designed chemicals, to properly address the synthesis of more effective derivatives. It is interesting to note that the model predicts good photodynamic activity for compound **35**, a hydroxy-substituted diarylchlorin, structurally similar to our most active compounds **18** and **19**. This prediction is confirmed by the in vivo and in vitro activity reported by the authors, who found that **35** was as effective as temoporfin **34** in their experimental model.[6b] [Note: While this paper was under revision, we have synthesized the unprecedented monoarylporphyrin **37**, which was among the novel photosensitizers hypothesized whose activity was predicted by the QSAR model. Experimental evaluation of the photodynamic activity of compound **37** on HCT 116 cells yielded an IC_{50} value (1.11 nM) very similar to the value predicted by the model (1.04 nM). This new result strengthens our feeling that the QSAR model, obtained from the set of molecules indicated, has very good predictivity and therefore could be applied to the screening of large sets of molecules belonging to the mono-, di-, and tetraaryl-substituted porphyrin class.]

Principal component analysis (PCA) of the three molecular descriptors of the proposed model was performed and is reported in Figure 7, where the chemicals (the points) are plotted in the descriptors space (the arrows for the loadings) of the two PCs most highly correlated with the response (respectively PC2, 85.5%, and PC3, 32.6%).

The explained variance of the molecular descriptors in these two PCs is 29.1% and 20.1%, respectively. PC1, while explaining 50.8% of the molecular descriptor variance, is the least correlated with the response (−7.8%). The chemicals are clearly separated along PC2 (related inversely to PW3 and directly to the other two descriptors) according to their degree of aryl substitution and activity (Figure 7A). As PC2 and PC3 correlate positively with the response, obviously with the corresponding weight (PC2 about three times more important than PC3), the chemicals on the left, and particularly at the bottom, have the lowest log $1/IC_{50}$ values. These compounds are the least active and belong to the series of tetraarylporphyrins; however, it is important to note that compound **34** (temoporfin, already used in clinical practice) is predicted as the most active tetraaryl-substituted porphyrin. Mono- and diaryl derivatives, generally more active than tetraarylporphyrins, are on the upper right side of the graph. Moreover, when the diarylporphyrin panel is considered, phenyl- or hydroxyphenyl-substituted compounds (dotted ellipse) show higher activity than the majority of methoxypheny- diarylporphyrins (solid circle), compound **20** being the only exception (as evident in the expanded portion of panel A plotted in panel B). Notably, among all the PSs examined in the present study, **20** is the only diaryl derivative featuring hydroxyl groups on 3,4,5 positions of one phenyl ring, and this structural difference with respect to the other hydroxy diaryl compounds is well highlighted by the descriptor space of the proposed model.

In Figure 7A, the predicted chemicals **35**−**41** are also plotted in the same molecular descriptor space. Application of the QSAR model to novel hypothetical derivatives (**37**−**41**), belonging to the chemical domain of the model, predicts a higher photodynamic activity for monoaryl- (**37**−**39**) than for diarylporphyrins (**40**, **41**), suggesting that synthesis of this class of compounds might be worth pursuing.

Conclusions

The results obtained in the present study suggest that diaryltetrapyrrole compounds are more effective that the corresponding tetraaryl derivatives in inducing photodynamic cell kill of human colon adenocarcinoma cells and that hydroxy-substituted compounds are more active than methoxy-substituted derivatives. The unintended isolation of three monoarylporphyrins as side products of the 5,15-diarylporphyrin synthesis allowed us to investigate their phototoxicity on HCT116 cells and to include them in the QSAR analysis: these molecules

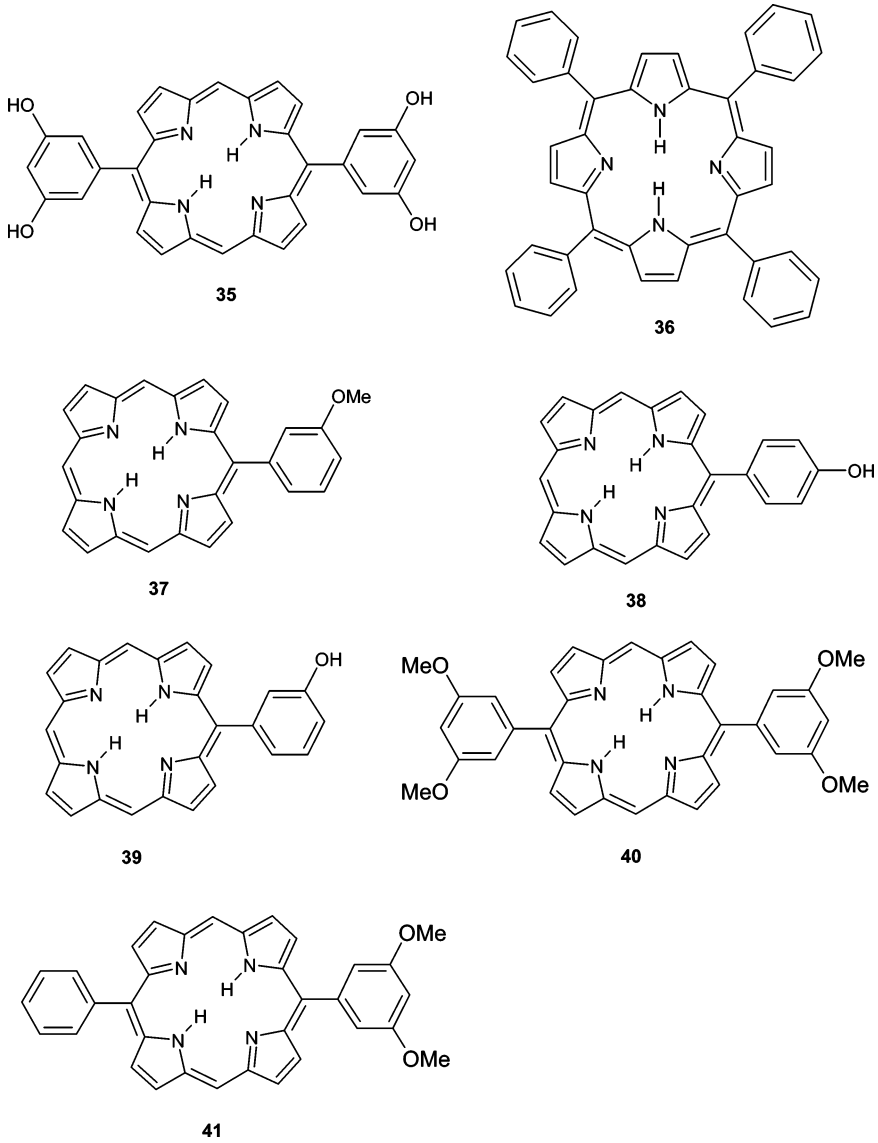

Figure 6. Structures of the seven molecules included in the QSAR model as "unknown" and predicted.

proved to be particularly promising photosensitizers, with IC_{50} values comparable to, or even better than, the most active diarylporphyrins.

QSAR studies performed on a representative set of PSs support this conclusion: a good predictive QSAR model, statistically externally validated and based on three theoretical molecular descriptors, was developed and allows for reliable predictions about the activity of seven PSs that were not experimentally tested in the present study, directing the synthesis of future potential PSs toward diaryl- or monoaryltetrapyrrolic compounds.

Interestingly, some of the new molecules (**19**, **21**, **22**, and **23**) were found to be more active than the clinically approved PSs porfimer sodium and temoporfin, at least in the in vitro model adopted in this study. However, in vivo studies are required to establish the actual therapeutic potential of these PSs and to significantly compare their pharmacodynamic/pharmacokinetic profiles with those of the agents already in clinical use for PDT.

Experimental Section

Chemistry. UV−vis absorption spectra were measured on a Perkin-Elmer Lambda 10 instrument. ^{1}H NMR spectra were recorded on a Bruker 400 MHz spectrometer in $CDCl_3$ or deuterated dimethyl sulfoxide (DMSO-d_6); chemical shifts are expressed in parts per million (ppm) relative to chloroform (7.28) and are reported as s (singlet), d (doublet), t (triplet), m (multiplet), or br s (broad singlet). Mass spectrometric measurements were performed on a Finnigan LCQ-MS instrument. Elemental analyses were performed on a ThermoQuest NA 2100 C, H, N analyzer, equipped with an electronic mass flow control and thermal conductivity detector. Analytical thin-layer chromatography (TLC) was performed on Merck 60 F254 silica gel (precoated sheets, 0.2 mm thick). Silica gel 60 (70−230 mesh, Merck) was used for column chromatography. Aromatic aldehydes were commercial products (Sigma−Aldrich) and were used as received. Pyrrole and $BF_3{\cdot}Et_2O$ were freshly distilled prior to use. Dichloromethane used for porphyrin synthesis was distilled from $CaCl_2$ directly into the reaction flask.

Synthesis of Free Base Tetraarylporphyrins. 5,10,15-Triphenyl-20-(4-methoxyphenyl)-21*H*,23*H*-porphyrin **1**, 5,10,15-triphenyl-20-(3-methoxyphenyl)-21*H*,23*H*-porphyrin **2**, 5,10,15-triphenyl-20-(3,4,5-trimethoxyphenyl)-21*H*,23*H*-porphyrin **3**, and 5,10,15-tri-(4-methoxyphenyl)-20-(3,4,5-trimethoxyphenyl)-21*H*,23*H*-porphyrin **4** were synthesized via condensation of the corresponding aromatic aldehydes and pyrrole under mixed-acid catalysis, as recently reported by Lindsey and co-workers.[9] The general procedure for porphyrin synthesis is fully described for the first compound, the others being prepared under similar conditions.

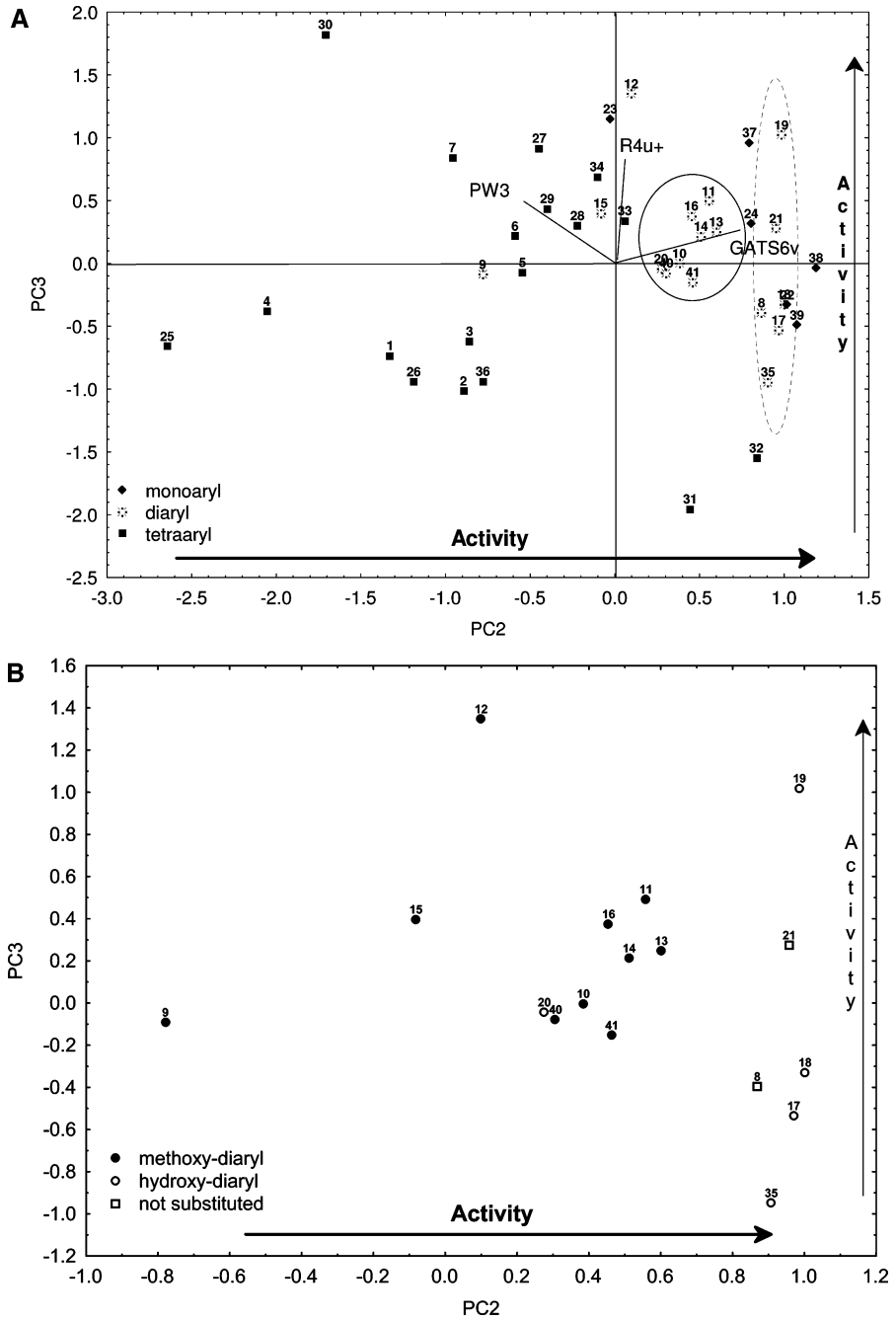

Figure 7. (A) Loadings and score plots from principal component analysis (PCA: PC2−PC3) of the three molecular descriptors of the proposed QSAR model for log ($1/IC_{50}$). (B) Enlarged view of PCA from panel A only for diarylporphyrins: methoxy-, hydroxyl-, and nonsubstituted derivatives are differently labeled.

5,10,15-Triphenyl-20-(4-methoxyphenyl)-21*H*,23*H*-porphyrin (1). $BF_3{\cdot}Et_2O$ (12 μL, 1.2×10^{-2} mmol) and 0.35 mL (4.5 mmol) of trifluoroacetic acid (TFA) were added to a solution of 0.379 mL (3.75 mmol) of benzaldehyde, 0.152 mL (1.25 mmol) of *p*-anisaldehyde, and 0.35 mL (5 mmol) of freshly distilled pyrrole in 500 mL of CH_2Cl_2; the mixture was kept at room temperature for 2 h. The reaction was controlled over time by TLC (SiO_2; hexane/CH_2Cl_2 = 1/1). Then 570 mg (3.73 mmol) of DDQ was added when the aldehydes were completely reacted, and the mixture was kept at room temperature for 2 h. The solvent was evaporated and the crude product was purified by column chromatography (SiO_2; CH_2Cl_2/hexane 6/4). Three different compounds were separated: 5,10,15,20-tetraphenyl-21*H*,23*H*-porphyrin, 110 mg (14.3%); 5,10-diphenyl-15,20-(4-methoxyphenyl)-21*H*,23*H*-porphyrin, 55 mg (6.4%); and the desired product 5,10,15-triphenyl-20-(4-methoxyphenyl)-21*H*,23*H*-porphyrin, 140 mg (17.4%); R_f 0.63 (SiO_2; CH_2Cl_2/hexane = 6/4); MS-ESI$^+$ *m*/*z* 645.4 (M + 1) (100%). Anal. Calcd for ($C_{45}H_{32}N_4O$): C, H, N.

5,10,15-Triphenyl-20-(3-methoxyphenyl)-21*H*,23*H*-porphyrin (2). Compound **2** was synthesized as described above. Three different compounds were separated: 5,10,15,20-tetraphenyl-21*H*,-23*H*-porphyrin, 110 mg (14.3%); 5,10-diphenyl-15,20-(3-methoxyphenyl)-21*H*,23*H*-porphyrin, 150 mg (17.5%); and the desired product 5,10,15-triphenyl-20-(4-methoxyphenyl)-21*H*,23*H*-porphyrin, 125 mg (19%); R_f 0.35 (SiO_2; CH_2Cl_2/hexane = 1/1); MS-ESI$^+$ *m*/*z* 645.4 (M + 1) (100%). Anal. Calcd for ($C_{45}H_{32}N_4O$): C, H, N.

5,10,15-Triphenyl-20-(3,4,5-trimethoxyphenyl)-21*H*,23*H*-porphyrin (3). 3,4,5-Trimethoxybenzaldehyde (245.5 mg, 1.25 mmol), 0.380 mL (3.75 mmol) of benzaldehyde, and 0.35 mL (5 mmol) of pyrrole were reacted as described for compound **1**. The crude material was purified by means of two subsequent column chro-

matographies (SiO_2; CH_2Cl_2/hexane = 1/1). The total amount of **3**, isolated as pure product, was 150 mg (0.21 mmol, 16.8%); R_f 0.32 (SiO_2; CH_2Cl_2/hexane = 1/1); MS-ESI$^+$ *m*/*z* 705.2 (M + 1) (100%). Anal. Calcd for ($C_{47}H_{36}N_4O_3$): C, H, N. In addition to **3**, 380 mg (0.62 mmol, 49%) of 5,10,15,20-tetraphenyl-21*H*,23*H*-porphyrin was also recovered from the reaction.

5,10,15-Tri-(4-methoxyphenyl)-20-(3,4,5-trimethoxyphenyl)-21*H*,23*H*-porphyrin (4). 3,4,5-Trimethoxybenzaldehyde (245.5 mg, 1.25 mmol), 0.426 mL (3.75 mmol) of *p*-anisaldehyde, and 0.35 mL (5 mmol) of pyrrole were reacted as described for compound **1**. The crude product was purified by means of two subsequent column chromatographies (SiO_2; CH_2Cl_2); 100 mg (14%) of **3** was isolated as pure product; R_f 0.3 (SiO_2; CH_2Cl_2; MS-ESI$^+$ *m*/*z* 795.2 (M + 1) (100%). Anal. Calcd for ($C_{50}H_{42}N_4O_6$): C, H, N. From this reaction was also isolated 95 mg (10.2%) of 5,10,15,20-tetra-(4-methoxyphenyl)-21*H*,23*H*-porphyrin as secondary product.

Synthesis of Free Base Diarylporphyrins. The general procedure for porphyrin syntheses is fully described for the first compound, the others being prepared under similar conditions.

5,15-Diphenyl-21*H*,23*H*-porphyrin (8). TFA (0.168 mL, 2.18 mmol) was added to a solution of 0.275 mL (2.72 mmol) of benzaldehyde and 398 mg (2.72 mmol) of 2,2′-dipyrromethane in 400 mL of CH_2Cl_2; the mixture was kept at room temperature for 2 h. The disappearance of the aldehyde from the reaction mixture was determined by TLC (SiO_2; CH_2Cl_2); then 650 mg (2.86 mmol) of DDQ was added and the mixture was kept at room temperature for 2 h. The solvent was evaporated and the crude product was purified by column chromatography (SiO_2; hexane/CH_2Cl_2 = 1/1). Two fractions were collected: the first was 5-monophenyl-21*H*,23*H*-porphyrin **22** (14 mg, 2.6%), and the second was the desired product.

5,15-Diphenyl-21*H*,23*H*-porphyrin 8: 158 mg (25%); R_f 0.56 (SiO_2; hexane/CH_2Cl_2 = 1/1); MS-ESI$^+$ *m*/*z* 463.1 (M + 1) (100%). Anal. Calcd for ($C_{32}H_{22}N_4$): C, H, N.

5-Monophenyl-21*H*,23*H*-porphyrin 22: R_f 0.76 (SiO_2; hexane/CH_2Cl_2 1/1); MS-ESI$^+$ *m*/*z* 387.2 (M + 1) (100%). Anal. Calcd for ($C_{26}H_{18}N_4$): C, H, N.

5,15-Di-(4-methoxyphenyl)-21*H*,23*H*-porphyrin (9). To a solution of 0.242 mL (2.12 mmol) of *p*-anisaldehyde and 310 mg (2.12 mmol) of 2,2′-dipyrromethane in 500 mL of CH_2Cl_2 was added 0.038 mL (0.30 mmol) of $BF_3{\cdot}Et_2O$; the mixture was then treated with 502 mg (2.22 mmol) of DDQ and worked up as described above. The crude product was purified by column chromatography (SiO_2; CH_2Cl_2/hexane/AcOEt = 20/3/2). The product was further purified with a second column chromatography (SiO_2; CH_2Cl_2/hexane = 6/4). Two fractions were recovered: the first was 5-mono-(4-methoxyphenyl)-21*H*,23*H*-porphyrin **23** (16 mg, 3.6%), and the second was the desired product (45 mg, 8%).

5,15-Di-(4-methoxyphenyl)-21H,23H-porphyrin 9: R_f 0.48 (SiO_2; hexane/CH_2Cl_2 = 6/4); MS-ESI$^+$ *m*/*z* 523.1 (M + 1) (100%). Anal. Calcd for ($C_{34}H_{26}N_4O_2$): C, H, N.

5-Mono-(4-methoxyphenyl)-21*H*,23*H*-porphyrin 23: R_f 0.69 (SiO_2; hexane/CH_2Cl_2 = 6/4); MS-ESI$^+$ *m*/*z* 417 (M + 1) (100%). Anal. Calcd for ($C_{27}H_{20}N_4O$): C, H, N.

5,15-Di-(3-methoxyphenyl)-21*H*,23*H*-porphyrin (10). 3-Methoxybenzaldehyde (0.330 mL, 2.72 mmol), 398.5 mg (2.72 mmol) of 2,2′-dipyrromethane, and 0.168 mL of TFA were reacted as described for compound **8**. The crude product was purified by column chromatography (SiO_2; CH_2Cl_2) and the recovered product was crystallized by dissolving the solid in the minimum amount of dichloromethane and then settling as a precipitate by careful addition of hexane. Compound **10** (145 mg, 20%) was isolated as pure product: R_f 0.72 (SiO_2; CH_2Cl_2); MS-ESI$^+$ *m*/*z* 523.1 (M + 1) (100%). Anal. Calcd for ($C_{34}H_{26}N_4O_2$): C, H, N.

5,15-Di-(3,4,5-trimethoxyphenyl)-21*H*,23*H*-porphyrin (11). A solution of 980 mg (5 mmol) of 3,4,5-trimethoxybenzaldehyde and 750 mg (5 mmol) of 2,2′-dipyrromethane in 500 mL of CH_2Cl_2 were treated with 0.094 mL (0.75 mmol) of $BF_3{\cdot}Et_2O$; the addition of DDQ (1186 mg 5.25 mmol) allows the oxidation of porphyrinogen. The crude product was purified by column chromatography (SiO_2; CH_2Cl_2/hexane/Et_2O = 20/3/2). Two fractions were recovered: the first was 5-mono-(3,4,5-trimethoxyphenyl)-21*H*,23*H*-porphyrin **24** (184 mg, 20%), and the second was the desired product (176 mg, 11%).

5,15-Di-(3,4,5-trimethoxyphenyl)-21*H*,23*H*-porphyrin 11: R_f 0.54 (SiO_2; CH_2Cl_2/hexane/Et_2O = 20/3/2); MS-ESI$^+$ *m*/*z* 643.2 (M + 1) (100%). Anal. Calcd for ($C_{38}H_{34}N_4O_6$): C, H, N.

5-Mono-(3,4,5-trimethoxyphenyl)-21*H*,23*H*-porphyrin 24: R_f 0.75 (SiO_2; CH_2Cl_2/hexane/Et_2O = 20/3/2); MS-ESI$^+$ *m*/*z* 477.2 (M + 1) (100%). Anal. Calcd for ($C_{29}H_{24}N_4O_3$): C, H, N.

5-Phenyl-15-(4-methoxyphenyl)-21*H*,23*H*-porphyrin (12). TFA (0.215 mL, 2.18 mmol) and 5.4 μL of $BF_3{\cdot}Et_2O$ were added to a 500 mL of CH_2Cl_2 solution containing 0.173 mL (1.71 mmol) of benzaldehyde, 0.208 mL (1.71 mmol) of *p*-anisaldehyde, and 500 mg (3.42 mmol) of 2,2′-dipyrromethane. The oxidation was obtained with 780 mg (3.59 mmol) of DDQ. Compound **12** (80 mg, 16%) was obtained after two subsequent chromatographies (SiO_2; CH_2Cl_2 and CH_2Cl_2/hexane = 6:4): R_f 0.52 (SiO_2; CH_2Cl_2/hexane = 6/4); MS-ESI$^+$ *m*/*z* 493.3 (M + 1) (100%). Anal. Calcd for ($C_{33}H_{24}N_4O$): C, H, N. In addition to the desired product, 55 mg (8.3%) of 5,15-diphenyl-21*H*,23*H*-porphyrin **8** was also isolated as secondary product.

5-Phenyl-15-(3-methoxyphenyl)-21H,23H-porphyrin (13). Compound **13** was synthesized from *m*-anisaldehyde and benzaldehyde as described in the case of compound **12**. The isolated pure product was 100 mg (20% yield): R_f 0.55 (SiO_2; CH_2Cl_2/hexane = 6/4); MS-ESI$^+$ *m*/*z* 493.3 (M + 1) (100%). Anal. Calcd for ($C_{33}H_{24}N_4O$): C, H, N. In this reaction, 80 mg (12.1%) of 5,15-diphenyl-21*H*,23*H*-porphyrin was also isolated.

5-Phenyl-15-(3,4,5-trimethoxyphenyl)-21*H*,23*H*-porphyrin (14). The title compound was synthesized from 0.140 mL (1.36 mmol) of benzaldehyde and 266 mg (1.36 mmol) of 3,4,5-trimethoxybenzaldehyde as described above and was isolated in 4% yield (38 mg) after two column chromatographies: R_f 0.35 (SiO_2; CH_2Cl_2/hexane = 6/4); MS-ESI$^+$ *m*/*z* 553.2 (M + 1) (100%). Anal. Calcd for ($C_{35}H_{28}N_4O_3$): C, H, N.

5-(3,4,5-trimethoxyphenyl)-15-(4-methoxyphenyl)-21*H*,23*H*-porphyrin (15). 4-Methoxybenzaldehyde (0.270 mL, 2.22 mmol), 3,4,5-trimethoxybenzaldehyde (436.1 mg, 2.22 mmol), 650 mg (4.44 mmol) of 2,2′-dipyrromethane, 0.279 mL of TFA, and 7 μL (0.056 mmol) of $BF_3{\cdot}Et_2O$ were reacted as described for compound **8**. The crude material was purified by column chromatography (SiO_2; CH_2Cl_2) affording 200 mg (14%) of pure product **15**: R_f 0.44 (SiO_2; CH_2Cl_2); MS-ESI$^+$ *m*/*z* 583.3 (M + 1) (100%). Anal. Calcd for ($C_{35}H_{30}N_4O_4$): C, H, N. In addition to compound **15**, 90 mg (9.7%) of porphyrin **9** was also isolated from the mixture.

5-(3,4,5-Trimethoxyphenyl)-15-(3-methoxyphenyl)-21*H*,23*H*-porphyrin (16). Compound **16** was synthesized as described for compound **15**, and the isolated pure product yield was 65 mg (11%): R_f 0.46 (SiO_2; CH_2Cl_2); MS-ESI$^+$ *m*/*z* 583.3 (M + 1) (100%). Anal. Calcd for ($C_{35}H_{30}N_4O_4$): C, H, N. From the reaction mixture, 15 mg (1.6%) of compound **10** was also recovered.

Synthesis of Hydroxy-Substituted Porphyrins from Methoxyporphyrins. Porphyrins bearing hydroxyls as substituents on *meso*-phenyls were obtained by demethylation of corresponding methoxy groups, following the BBr_3 general method.[34]

5,10,15-Triphenyl-20-(4-hydroxyphenyl)-21*H*,23*H*-porphyrin (5). A solution of 80 mg (0.124 mmol) of porphyrin **1** in 15 mL of CH_2Cl_2 was stirred at 0 °C for 15 min, and then 2.48 mL (2.48 mmol) of 1 M BBr_3 dichloromethane solution was added. The mixture was kept at 0 °C for 1 h and at room temperature for 18 h; after this period, 30 mL of CH_2Cl_2 was added to the reaction flask together with the desired amount of Na_2CO_3 saturated solution to neutralize the mixture. The layers were separated and the organic phase was thoroughly washed with water, dried (Na_2SO_4), and concentrated to dryness, yielding **5** as solid pure product after crystallization (65 mg, 83%): R_f 0.38 (SiO_2; CH_2Cl_2); MS-ESI$^+$ *m*/*z* 631.4 (M + 1) (100%). Anal. Calcd for ($C_{44}H_{30}N_4O$): C, H, N.

5,10,15-Triphenyl-20-(3-hydroxyphenyl)-21*H*,23*H*-porphyrin (6). A solution of 70 mg (0.108 mmol) of porphyrin **2** in 20 mL of CH_2Cl_2 was treated with 2.16 mL (2.16 mmol) of 1 M BBr_3

solution. The isolated pure product yield was 47 mg (69%): R_f 0.53 (SiO_2; CH_2Cl_2); MS-ESI$^+$ *m*/*z* 631.4 (M + 1) (100%). Anal. Calcd for ($C_{44}H_{30}N_4O$): C, H, N.

5,10,15-Triphenyl-20-(3,4,5-hydroxyphenyl)-21*H*,23*H*-porphyrin (7). A solution of 40 mg (0.056 mmol) of porphyrin **4** in 25 mL of CH_2Cl_2 was treated with 2.0 mL (2.0 mmol) of BBr_3 solution. The isolated pure product yield was 30 mg (75%): R_f 0.21 (SiO_2; CH_2Cl_2); MS-ESI$^+$ *m*/*z* 663.2 (M + 1) (100%). Anal. Calcd for ($C_{44}H_{30}N_4O_3$): C, H, N.

5,15-Di-(3-hydroxyphenyl)-21*H*,23*H*-porphyrin (17). BBr_3 1 M dichloromethane solution (1.57 mL, 1.57 mmol) was added to a solution of 41 mg (0.078 mmol) of porphyrin **10** in 10 mL of CH_2Cl_2. After crystallization, 18 mg (46%) of **17** was isolated: R_f 0.32 (SiO_2; CH_2Cl_2); MS-ESI$^+$ *m*/*z* 495.2 (100%). Anal. Calcd for ($C_{32}H_{22}N_4O_2$): C, H, N.

5-Phenyl-15-(4-hydroxyphenyl)-21*H*,23*H*-porphyrin (18). A solution of 50 mg (0.101 mmol) of porphyrin **12** in 5 mL of CH_2Cl_2 was treated with 3.03 mL (3.03 mmol) of BBr_3 solution, and 30 mg (62.5%) of pure compound **18** was isolated: R_f 0.37 (SiO_2; CH_2Cl_2); MS-ESI$^+$ *m*/*z* 479.1 (M + 1) (100%). Anal. Calcd for ($C_{32}H_{22}N_4O$): C, H, N.

5-Phenyl-15-(3-hydroxyphenyl)-21*H*,23*H*-porphyrin (19). A solution of 60 mg (0.12 mmol) of porphyrin **13** in 15 mL of CH_2Cl_2 was treated with 2.5 mL (2.5 mmol) of BBr_3 solution, and 36 mg (62%) of the desired product was recovered: R_f 0.38 (SiO_2; CH_2Cl_2); MS-ESI$^+$ *m*/*z* 479.1 (M + 1) (100%). Anal. Calcd for ($C_{32}H_{22}N_4O$): C, H, N.

5-Phenyl-15-(3,4,5-trihydroxyphenyl)-21*H*,23*H*-porphyrin (20). A solution of 20 mg (0.036 mmol) of porphyrin **14** in 25 mL of CH_2Cl_2 was treated with 2 mL (2 mmol) of BBr_3 solution. The isolated pure product was 15 mg, corresponding to 81% yield: R_f 0.26 (SiO_2; CH_2Cl_2); MS-ESI$^+$ *m*/*z* 511.4 (M + 1) (100%). Anal. Calcd for ($C_{32}H_{22}N_4O_3$): C, H, N.

Synthesis of Chlorin from Porphyrin: 5,10-Diphenyl-21*H*,-23*H*-chlorin (21). Toluene-4-sulfonylhydrazide (128 mg, 0.688 mmol) and 475.4 mg (3.44 mmol) of K_2CO_3 were added to a solution of 40 mg (0.086 mmol) of 5,15-diphenyl-21*H*,23*H*-porphyrin **8** in 6 mL of pyridine, and then the mixture was refluxed for 2 h; the reaction progress was monitored by means of UV−vis spectroscopy, based on the occurrence of the chlorin absorption band at 650 nm. Equivalent amounts of hydrazide and K_2CO_3 were added every hour until the reaction was completed (determined by evaluating the ratio of the intensity between the band at 400 nm and that at 650 nm; this ratio must be equal or lower than 6). At the end of the reaction, 10 mL of AcOEt and 20 mL of H_2O were added and the mixture was kept at 70 °C for 1 h. Afterward the organic layer was separated, washed a few times with 10% HCl and then with H_2O, and finally dried (Na_2SO_4). Solvent evaporation under vacuum afforded chlorin **21** as a solid product (24 mg, 59%). Once more the absorption spectrum of the isolated compound was controlled; the presence of the peak at 730 nm indicates the formation of some overreduction product (bacteriochlorin); the crude solid was then dissolved in CH_2Cl_2 and treated with a diluted toluene solution of chloranyl. This procedure must be carried out with particular attention to avoid oxidation of the chlorin back to the initial porphyrin. As the final step of the reaction, the solution was concentrated and purified by column chromatography (SiO_2; hexane/CH_2Cl_2 = 1/1) to give 15 mg (37%) of the pure product: R_f 0.54 (SiO_2; hexane/CH_2Cl_2 = 1/1); MS-ESI$^+$ *m*/*z* 465.1 (M + 1) (100%). Anal. Calcd for ($C_{32}H_{22}N_4$): C, H, N.

Photobleaching Measurements. About 0.2 mL of DMSO porphyrin mother solution was diluted to 15 mL with 0.1 M phosphate-buffered saline (PBS) in order to obtain a 5×10^{-5} M porphyrin concentration. This solution was exposed at 37 °C to a 500 W tungsten−halogen lamp fitted with aqueous filter for 2 h.. Every 15 min, 0.4 mL samples were withdrawn and diluted with 1.6 mL of PBS, and their UV−vis absorption was measured.

Cytotoxicity Studies. Human adenocarcinoma HCT116 cells were obtained from the American Type Culture Collection (Rockville, MD) and maintained in Dulbecco's modified Eagle medium (DMEM; Mascia-Brunelli, Milano, Italy) supplemented with 10% fetal bovine serum (Mascia-Brunelli) at 37 °C in a humidified 5% CO_2 atmosphere. The antiproliferative effect of the different PS was assessed by the model transformation tools (MTT) assay.[35] Briefly, 5×10^4 cells/mL were seeded onto 96-well plates and allowed to grow for 48 h prior to treatment with different PS concentrations. After 24 h, the PS-containing medium was replaced by PBS, and cells were irradiated under visible light (tungsten−halogen lamp 500 W) for 2 h (average value between 380 and 780 nm determined with a Licor-1800 spectroradiometer; light irradiance 22 mW/cm^2 and a light energy of 158.4 J/cm^2). At the end of this time, cells were incubated for 24 h at 37 °C in drug-free medium; MTT was then added to each well (final concentration 0.4 mg/mL) for 3 h at 37 °C and formazan crystals formed through MTT metabolism by viable cells were dissolved in dimethyl sulfoxide (DMSO). Optical densities were measured at 570 nm by use of a Universal Microplate Reader EL800 (Bio-Tek Instruments).

Possible intrinsic (i.e., nonphotodynamic) cytotoxic effects of the PS were assessed on control cells treated as described above, with PS concentrations up to 10-fold higher than those used for PDT experiments, omitting cell irradiation.

IC_{50} (i.e., the concentration affecting 50% of cells) values were obtained by nonlinear regression analysis, using the GraphPad PRISM 3.03 software (GraphPad Software Inc., San Diego, CA)

QSAR: Experimental Data Set. The IC_{50} values, expressed in nanomolar concentrations, used to develop the QSAR model were obtained from this work (24 data) and from previously reported results (10 data).[7] The final set consists of IC_{50} values of 34 PSs expressed as log $1/IC_{50}$.

In Supporting Information are reported experimental and predicted data (Table 3) and the structures of the 10 photosensitizerss previously synthesized (Figure 1).

Molecular Descriptors. The geometries of the 41 studied porphyrins were fully optimized without constraints by use of the semiempirical quantum-mechanical PM3 Hamiltonian as implemented in HYPERCHEM[22] as molecular modeling software. The three-dimensional structures of minimum energy conformation were used as input for the DRAGON software,[21] which was employed to numerically encode the topology and geometry of these molecules by theoretical molecular descriptors. A total of about 1200 molecular descriptors of different kinds (mono-, bi-, and three-dimensional) were calculated to describe compound chemical diversity.

To compare the modeling power of variables, traditionally used to model biological end points, with the above-listed theoretical molecular descriptors, different kinds of log *P* (calculated values for *A* log *P*,[21] *M* log *P*,[21] and HYPER-log *P*[22]) were used. Quantum-chemical descriptors such as HOMO (highest occupied molecular orbital), LUMO (lowest unoccupied molecular orbital), HOMO−LUMO gap (DHL), the ionization potential (P_{ion}) and the heat of formation (*H*), calculated by the semiempirical PM3 Hamiltonian for the geometry optimization method available in the HYPERCHEM package,[22] were always added and used for descriptor selection during model development.

Constant values and descriptors found to be correlated pairwise were excluded in a prereduction step (when there was more than 98% pairwise correlation, one variable was deleted), and the genetic algorithm was applied for variable selection to a final set of about 270 descriptors.

The values of the selected molecular descriptors are reported in Table 3 of Supporting Information.

Chemometric Methods. Multiple linear regression (MLR) and genetic algorithm-−variable subset selection (GA-VSS)[23] were performed by the software *MOBY DIGS* of Todeschini et al.[36] using the ordinary least-squares regression (OLS) method, optimizing the prediction power Q^2_{loo} (leave-one-out procedure). This algorithm provides the subsets of the most predictive molecular descriptors for the selected property, automatically chosen among all the available descriptors.

To avoid multicollinearity with or without "apparent" prediction power (chance correlation), the regressions were calculated only for variable subsets with an acceptable multivariate correlation with response, by applying the QUIK rule (*Q* under influence of *K*),[37]

which does not consider models with a K multivariate correlation index of the $[X]$ variable block greater than the correlation within the $[X + y]$ block variables, where X is the molecular descriptors and y is the response variable.

In the MLR equation of the model, reported in this paper, the variables are listed in order of relative importance by their standardized regression coefficients. In fact, since molecular descriptors do not have equal variance (i.e., they are not autoscaled), their relative importance in the model is measured better by standardized regression coefficients (i.e., the coefficients multiplied by the standard deviation of the corresponding predictor). The errors of the regression coefficients have also been reported for each equation.

Validation. The robustness of the models and their predictivity were evaluated by both Q^2_{loo} and bootstrap. In this last procedure K n-dimensional groups are generated by a randomly repeated selection of n objects from the original data set. The model obtained on the first selected objects is used to predict the values for the excluded sample and then Q^2 is calculated for each model. The bootstrapping was repeated 5000 times for each validated model.

The proposed models are also checked for reliability and robustness by permutation testing;[32] new models are recalculated for randomly reordered response (Y scrambling) in order to exclude by chance models.

The actual predictive capability of each model developed on the training set is verified on an external validation set[24] and is calculated from $Q^2_{ext} = 1 - \text{PRESS/SD}$, where PRESS is the sum of squared differences between the measured response and the predicted value for each molecule in the validation set, and SD is the sum of squared deviations between the measured response for each molecule in the validation set and the mean measured value of the training set. A measure to define the accuracy of the proposed QSARs is also the RMSE (root mean square of errors) that summarizes the overall error of the model. It is calculated as the root square of the sum of the squared errors in predictions divided by their total number (RMSE and RMSEP, calculated separately for the training and the test/validation sets):

$$\text{RMSE} = \sqrt{\frac{\sum_i (y_i - \hat{y}_i)^2}{n}}$$

Splitting Training/Test for External Validation. To have compounds for external validation, the original data set of 34 compounds was split into a training set and an external validation set. The splitting of the data set was realized considering the distribution of the response value: $^2/_3$ of the studied compounds (22 objects) were selected as a training set and used for the model developing, and the remaining 12 molecules were used as a validation set, to allow the external statistical validation of the model.

Chemical Domain. QSAR models must always be verified for their applicability with regard to chemical domain. The presence of outliers (i.e., compounds with cross-validated standardized residuals greater than 2.5 standard deviation units) and chemicals very structurally influential in determining model parameters [i.e., compounds with high *leverage* value (h)[33] greater than $3\,p'/n$ (h^*), where p' is the number of model variables plus one, and n is the number of the objects used to calculate the model] was also verified. The reliability of the predicted data with regard to chemical domain was verified by the *leverage* approach: the predictions for chemicals of the validation set with a leverage value smaller than h^* must be considered reliable, being into the structural chemical domain of the training set.

Principal component analysis (PCA) for data exploration was performed on autoscaled data by the *SCAN*[38] and *STATISTICA*[39] packages.

Supporting Information Available: Spectroscopic data (^{1}H NMR and UV−vis) and elemental analysis data for compounds **1**−**24**; structures of the 10 photosensitizers previously synthesized;[7] list of the calculated log P values (A log P, M log P, and HYPER-log P), molecular descriptors, and experimental and predicted log ($1/IC_{50}$) (IC_{50} in nanomolar). This material is available free of charge via the Internet at http://pubs.acs.org.

References

(1) Johnson, S.; Johnson F. N. *Reviews in Contemporary Pharmacotherapy−Photodynamic Therapy*; Marius Press: Carnforth, U.K., 1999.

(2) Macdonald, I. J.; Dougherty, T. J. Basic principles of photodynamic therapy. *J. Porphyrins Phthalocyanines* **2001**, *5* (2), 105−129.

(3) Lin, V. S.; Therien, M. J. The Role of Steric and Electronic Effects in the Extensive Modulation of the Absorptive and Emissive Properties of a Series of Ethynyl- and Butadiynyl-Bridged Bis- and Tris-Porphinato(zinc) Chromophores. *Chem. Eur. J.* **1995**, *1*, 645−651.

(4) Wang, Q. M.; Bruce, D. W. Low-Melting, Liquid-Crystalline Metalloporphyrins. *Angew. Chem., Int. Ed. Engl.* **1997**, *36*, 150−152.

(5) Osuka, A.; Shimidzu, H. *meso,meso*-Linked Porphyrin Arrays. *Angew. Chem., Int Ed. Engl.* **1997**, *36*, 135−137.

(6) (a) Macalpine, J. K.; Boch, R.; Dolphin, D. Evaluation of tetraphenyl-2,3-dihydroxychlorins as potential photosensitizers. *J. Porphyrins Phthalocyanines* **2002**, *6*, 146−155. (b) Bourré, L.; Simonneaux, G.; Ferrand, Y.; Thibaut, S.; Lajat, Y.; Patrice, T. Synthesis, and in vitro and in vivo evaluation of a diphenylchlorin sensitizer for photodynamic therapy. *J. Photochem. Photobiol. B: Biol.* **2003**, *69*, 179−192.

(7) Banfi, S.; Caruso, E.; Caprioli, S.; Mazzagatti, L.; Canti, G.; Ravizza, R.; Gariboldi, M.; Monti, E. Photodynamic effects of porphyrin and chlorin photosensitizers in human colon adenocarcinoma cells. *Bioorg. Med. Chem.* **2004**, *12*, 4853−4860.

(8) Osterloh, J.; Vicente, M. G. H. Mechanisms of porphyrinoid localization in tumors. *J. Porphyrins Phthalocyanine* **2002**, *6* (5), 305−324.

(9) Chevalier, F.; Geier, G. R., III; Lindsey, J. S. Acidolysis of intermediates used in the preparation of core-modified porphyrinic macrocycles. *J. Porphyrins Phthalocyanines* **2002**, *6* (3), 186−197.

(10) (a) Bruckner, C.; Posakony, J. J.; Johnson, C. K.; Boyle, R. W.; James, B. R.; Dolphin, D. Novel and improved synthesis of 5,15-diphenylporphyrin and its dipyrrolic precursors. *J. Porphyrins Phthalocyanines* **1998**, *2* (6), 455−465. (b) Clarke, O. J.; Boyle, R. W. Selective Synthesis of Asymmetrically Substituted 5,15-Diphenylporphyrins. *Tetrahedron Lett.* **1998**, *39*, 7167−7168.

(11) (a) Tamaru, S.; Yu, L.; Youngblood, J.; Muthukumaran, K.; Taniguchi, M.; Lindsey, J. S. A tin-complexation strategy for use with diverse acylation methods in the preparation of 1,9-diacyldipyrromethanes. *J. Org. Chem.* **2004**, *69*, 765−777. (b) Arumagam, N.; Won, D.; Lee, C. Synthesis of regioselectively functionalized, asymmetric porphyrins via "2+2" condensation. *J. Porphyrins Phthalocyanines* **2002**, *6* (7−8), 479−483.

(12) Plater, M. J.; Aiken, S.; Bourhill, G. A new synthetic route to donor−acceptor porphyrins. *Tetrahedron* **2002**, *58*, 2405−2413.

(13) Pandey, S. K.; Gryshuk, A. L.; Graham, A.; Ohkubo, K.; Fukuzumi, S.; Dobhal, M. P.; Zheng, G.; Ou, Z.; Zhan, R.; Kadish, K. M.; Oseroff, A.; Ramaprasad, S.; Pandey, R. K. Fluorinated photosensitizers: synthesis, photophysical, electrochemical, intracellular localization, in vitro photosensitizing efficacy and determination of tumor-uptake by ^{19}F in vivo NMR spectroscopy. *Tetrahedron* **2003**, *59*, 10059−10073.

(14) Bonnett, R.; White, R. D.; Winfield, U. J.; Berenbaum, M. C. Hydroporphyrins of the meso-tetra(hydroxyphenyl)porphyrin series as tumor photosensitizers. *Biochem. J.* **1989**, *261*, 277−280.

(15) (a) Bonnett, R.; Martinez, G. Photobleaching of sensitisers used in photodynamic therapy. *Tetrahedron* **2001**, *57*, 9513−9547. (b) Georgakoudi, I.; Foster, T. H. Singlet Oxygen- Versus Nonsinglet Oxygen-Mediated Mechanisms of Sensitizer Photobleaching and Their Effects on Photodynamic Dosimetry. *Photochem. Photobiol.* **1998**, *67*, 612−625.

(16) Bonnett, R.; Martinez, G. Photobleaching of compounds of the 5,10,15,20-tetrakis(*m*-hydroxyphenyl)-porphyrin series (m-THPP, m-THPC, and m-THPBC). *Org. Lett.* **2002**, *4* (12), 2013−2016.

(17) Henderson, B. W.; Bellnier, D. A.; Greco, W. R.; Sharma, A.; Pandey, R. K.; Vaughan, L. A.; Weishaupt, K. R.; Dougherty, T. J. An in vivo quantitative structure−activity relationship for a congeneric series of pyropheophorbide derivatives as photosensitizers for photodynamic therapy. *Cancer Res.* **1997**, *57*, 4000−4007.

(18) Potter, W. R.; Henderson, B. W.; Bellnier, D. A.; Pandey, R. K.; Vaughan, L. A.; Weishaupt, K. R.; Dougherty, T. J. Parabolic quantitative structure−activity relationships and photodynamic therapy: Application of a three-compartment model with clearance

to the in vivo quantitative structure−activity relationships of a congeneric series of pyropheophorbide derivatives used as photosensitizers for photodynamic therapy. *Photochem. Photobiol.* **1999**, *70*, 781−788.
(19) Vanyur, R.; Heberger, K.; Kovesdi, I.; Jakus, J. Prediction of tumoricidal activity and accumulation of photosensitizers in photodynamic therapy using multiple linear regression and artificial neural networks. *Photochem. Photobiol.* **2002**, *75*, 471−478.
(20) Debnath, A. K.; Jiang, S.; Strick, N.; Lin, K.; Haberfield, P.; Neurath, R. 3-Dimensional Structure−Activity Analysis of a series of Porphyrin Derivatives with Anti-HIV-1 Activity Targeted to the V3 Loop of the gp120 Envelope Glycoprotein of the Human-Immunodeficiency-Virus Type-1. *J. Med. Chem.* **1994**, *3*, 1099−1108.
(21) Todeschini, R.; Consonni, V.; Mauri, A.; Pavan, M. DRAGON Software for the Calculation of Molecular Descriptors, version 5.2 for Windows; Talete S.r.l.: Milan, Italy, 2005.
(22) HYPERCHEM/CHEMPLUS version 7.03 for Windows; Autodesk Inc.: Sausalito, CA, 2002.
(23) Leardi, R.; Boggia, R.; Terrile, M. Genetic Algorithms as a Strategy for Feature Selection. *J. Chemom.* **1992**, *6*, 267−281.
(24) Tropsha, A.; Gramatica, P.; Gombar, V. K. The Importance of Being Earnest: Validation is the Absolute Essential for Successful Application and Interpretation of QSPR Models. *QSAR Comb. Sci.* **2003**, *22*, 69−76.
(25) Geary, R. C. The contiguity ratio and statistical mapping, *Incorp. Statist.* **1954**, *5*, 115−145.
(26) Todeschini, R.; Consonni, V. *Handbook of Molecular Descriptors*; Wiley−VCH: Weinheim, Germany, 2000; p 667.
(27) Randic, M. Novel shape descriptors for molecular graphs. *J. Chem. Inf. Comput. Sci.* **2001**, *41*, 607−613.
(28) Consonni, V.; Todeschini, R.; Pavan, M. Structure/Response Correlation and Similarity/Diversity Analysis by GETAWAY descriptors. Part 1. Theory of the Novel 3D Molecular Descriptors. *J. Chem. Inf. Comput. Sci.* **2002**, *42*, 682−692.
(29) Renner, R. The *K*-ow controversy. *Environ. Sci. Technol.* **2002**, *36*, 410.
(30) Benfenati, E.; Gini, G.; Piclin, N.; Roncaglioni, A.; Vari, M. R. Predicting logP of pesticides using different software. *Chemosphere* **2003**, *53*, 1155−1164.
(31) Papa, E.; Villa, F.; Gramatica, P. Statistically Validated QSARs, Based on Theoretical Descriptors, for Modeling Aquatic Toxicity of Organic Chemicals in *Pimephales promelas* (Fathead Minnow). *J. Chem. Inf. Comput. Sci.* **2005**, *45*, 1256−1266.
(32) Eriksson, L.; Jaworska, J.; Worth, A.; Cronin, M.; McDowell, R. M.; Gramatica, P. Methods for Reliability, Uncertainty Assessment, and Applicability Evaluations of Regression Based and Classification QSARs. *Environ. Health Perspect.* **2003**, *111*, 1361−1375.
(33) Atkinson, A. C. *Plots, Transformation and Regression*; Clarendon Press: Oxford, U.K., 1985; p 282.
(34) Williard, P. G.; Fryhle, C. B. Boron Trihalide−Methyl Sulfide Complexes as for Dealkylation of Aryl Ethers. *Tetrahedron Lett.* **1980**, *21*, 3731−3734.
(35) Alley, M. C.; Scudiero, D. A.; Monks, A.; Hursey, M. L.; Czerwinski, M. J.; Fine, D. L.; Abbott, B. J.; Mayo, J. G.; Shoemaker, R. H.; Boyd, M. R. Feasibility of drug screening with panels of human tumor cell lines. *Cancer Res.* **1988**, *48*, 589−601.
(36) Todeschini R.; Ballabio D.; Consonni V.; Mauri A.; Pavan M. MOBY DIGS−Models By Descriptors In Genetic Selection, version 1 beta for Windows; Talete S.r.l.: Milan, Italy, 2004.
(37) Todeschini, R.; Maiocchi, A.; Consonni, V., The *K* correlation index: theory development and its application in chemometrics. *Chemom. Intell. Lab. Syst.* **1999**, *46*, 13−29.
(38) SCAN−−Software for Chemometric Analysis, version 1.1 for Windows; Minitab: State College, PA, 1995.
(39) *STATISTICA*, release 5.1 for Windows; StatSoft, Inc.: Tulsa, OK, 1987.

JM050997M